UNCLASSIFIED

Defense Technical Information Center
Compilation Part Notice

ADP013627

TITLE: Computational Constrains on Large Eddy Simulation of Inhomogeneous Turbulent Complex Geometry Flows

DISTRIBUTION: Approved for public release, distribution unlimited

This paper is part of the following report:

TITLE: DNS/LES Progress and Challenges. Proceedings of the Third AFOSR International Conference on DNS/LES

To order the complete compilation report, use: ADA412801

The component part is provided here to allow users access to individually authored sections of proceedings, annals, symposia, etc. However, the component should be considered within the context of the overall compilation report and not as a stand-alone technical report.

The following component part numbers comprise the compilation report:
ADP013620 thru ADP013707

UNCLASSIFIED

COMPUTATIONAL CONSTRAINS ON LARGE EDDY SIMULATION OF INHOMOGENEOUS TURBULENT COMPLEX GEOMETRY FLOWS

OLEG V. VASILYEV
Department of Mechanical and Aerospace Engineering,
University of Missouri-Columbia
Columbia, MO 65211, USA
VasilyevO@missouri.edu

1. Introduction

In large eddy simulation (LES) of turbulent flows the dynamics of the large scale structures are computed, while the effect of the small scale turbulence is modeled. The differential equations describing the space-time evolution of the large scale structures are formally derived by applying a low-pass filter with non-uniform filter width to the Navier-Stokes equations. For an incompressible flow the non-dimensional equations describing the evolution of large scale structures take the following form:

$$\frac{\partial \overline{u}_i}{\partial x_i} = -\left[\frac{\partial u}{\partial x_i}\right], \tag{1}$$

$$\frac{\partial \overline{u}_i}{\partial t} + \frac{\partial \overline{u_i u_j}}{\partial x_j} = -\frac{\partial \overline{p}}{\partial x_i} + \frac{1}{Re}\frac{\partial^2 \overline{u}_i}{\partial x_j \partial x_j} - \left[\frac{\partial u_i u_j}{\partial x_j} + \frac{\partial p}{\partial x_i} - \frac{1}{Re}\frac{\partial^2 u_i}{\partial x_j \partial x_j}\right], \tag{2}$$

where the square bracket denotes the commutation operator given by

$$\left[\frac{\partial F}{\partial x_i}\right] = \frac{\overline{\partial F}}{\partial x_i} - \frac{\partial \overline{F}}{\partial x_i}. \tag{3}$$

The filtered convective term $\overline{u_i u_j}$ is unknown in LES and is typically decomposed into the convective term $\overline{u}_i \overline{u}_j$ that can be computed and the remainder, called sub-grid scale (SGS) stress, which should be modelled:

$$\overline{u_i u_j} = \overline{u}_i \overline{u}_j - \underbrace{\left(\overline{u}_i \overline{u}_j - \overline{u_i u_j}\right)}_{\tau_{ij}}. \tag{4}$$

In order to derive LES equations from Eqs. (1), (2), and (4) the following three key assumptions are made:

1. The differentiation and filtering operations commute.
2. The shape of the low-pass filter is known.
3. The modeled subgrid scale stress corresponds to the low-pass filter used in deriving LES equations.

With these assumptions we obtain the classical LES equations

$$\frac{\partial \overline{u}_i}{\partial x_i} = 0, \tag{5}$$

$$\frac{\partial \overline{u}_i}{\partial t} + \frac{\partial \overline{u}_i \overline{u}_j}{\partial x_j} = -\frac{\partial \overline{p}}{\partial x_i} + \frac{1}{Re} \frac{\partial^2 \overline{u}_i}{\partial x_j \partial x_j} + \frac{\partial \tau_{ij}}{\partial x_j}. \tag{6}$$

Ironically, all three assumptions used in derivation of Eqs. (5)-(6) are very often violated, perhaps as a result of addressing other very important problems related to numerical methods. However, recent advancement in numerical algorithms and hardware, has necessitated a careful and systematic examination of this issue. The main objective of this paper is to present a way for LES to be consistent, *i.e.* satisfy all these assumptions.

2. Implicit Filtering

Due to the lack of a straightforward and robust filtering procedure for inhomogeneous flows, most large eddy simulations performed to date have not made use of explicit filtering. The nearly universal approach for LES in complex geometries is to argue that the finite support of the computational mesh together with the low-pass characteristics of the discrete differencing operators effectively act as a filter (Rogallo and Moin, 1984; Lund, 1997), *i.e.*

$$\left.\frac{\delta u}{\delta x}\right|_i = \frac{u_{i+1} - u_{i-1}}{2\Delta x} = \frac{d}{dx} \int_{x_{i-1}}^{x_{i+1}} u dx = \left.\frac{d\overline{u}}{dx}\right|_i, \tag{7}$$

where $\delta/\delta x$ and d/dx are respectively finite difference and the exact (analytical) derivative operators. This procedure is commonly referred as implicit filtering since an explicit filtering operation never appears in the solution procedure. Although the technique of implicit filtering has been used extensively in the past, there are several compelling reasons to adopt a more systematic approach. Foremost of these is the issue of consistency. While it is true that discrete derivative operators have a low-pass filtering effect, the associated filter acts only in one spatial direction in which the derivative is taken. This fact implies that each term in the Navier-Stokes equations is acted on by a distinct one-dimensional filter and the actual equations being

solved are

$$\frac{\partial \widetilde{\overline{u}_1}^{x_1}}{\partial x_1} + \frac{\partial \widetilde{\overline{u}_2}^{x_2}}{\partial x_2} + \frac{\partial \widetilde{\overline{u}_3}^{x_3}}{\partial x_3} = 0, \tag{8}$$

$$\frac{\partial \overline{u}_i}{\partial t} + \frac{\partial \widetilde{\overline{u}_i \overline{u}_1}^{x_1}}{\partial x_1} + \frac{\partial \widetilde{\overline{u}_i \overline{u}_2}^{x_2}}{\partial x_2} + \frac{\partial \widetilde{\overline{u}_i \overline{u}_3}^{x_3}}{\partial x_3} = -\frac{\partial \widetilde{\overline{p}}^{x_i}}{\partial x_i} + \frac{\partial \widetilde{\tau_{i1}}^{x_1}}{\partial x_1} + \frac{\partial \widetilde{\tau_{i2}}^{x_2}}{\partial x_2} + \frac{\partial \widetilde{\tau_{i3}}^{x_3}}{\partial x_3} + \frac{1}{Re}\left[\frac{\partial^2 \widehat{\overline{u}_i}^{x_1}}{\partial^2 x_1} + \frac{\partial^2 \widehat{\overline{u}_i}^{x_2}}{\partial^2 x_2} + \frac{\partial^2 \widehat{\overline{u}_i}^{x_3}}{\partial^2 x_3}\right], \tag{9}$$

where $\widetilde{(\cdot)}^{x_i}$ and $\widehat{(\cdot)}^{x_i}$ are the effective one-dimensional filters associated with the first and second difference operators respectively. Thus, there is no way to derive the discrete equations through the application of a single three-dimensional filter. Considering this ambiguity in the definition of the filter, it is nearly impossible to make detailed comparisons of LES results with filtered DNS or experimental data.

The second significant limitation of the implicit filtering approach is the inability to control numerical error. Without an explicit filter, there is no direct control of the energy in the high frequency portion of the spectrum. Significant energy in this portion of the spectrum coupled with the non-linearities in the Navier-Stokes equations can produce significant aliasing error. Furthermore, all discrete derivative operators become rather inaccurate for high frequency solution components and this error interferes with the dynamics of the small scale eddies. This error can be particularly harmful when the dynamic model is used (Germano *et al.*, 1991; Ghosal *et al.*, 1995), since it relies entirely on information contained in the smallest resolved scales.

3. Explicit Filtering

The difficulties associated with the implicit filtering approach can be alleviated by performing an explicit filtering operation as an integral part of the solution process (Ghosal, 1996; Vasilyev *et al.*, 1998). By damping the energy in the high frequency portion of the spectrum it is possible to reduce or eliminate the various sources of numerical error that dominate this frequency range. Explicit filtering reduces the effective resolution of the simulation, but allows the filter size and shape to be chosen independently of the mesh spacing. In addition explicit filtering provides the means for both assessing and minimizing the effects of numerical error in practical simulations.

In order to illustrate the explicit filtering procedure further, consider a discrete time integration applied to the LES Eqns. (5)-(6):

$$\overline{u}_i^{n+1} = \overline{u}_i^n + \Delta_L \overline{u}_i^{n+1} + \Delta_{NL} \overline{u}_i^{n+1}, \tag{10}$$

where $\Delta_L \overline{u}_i^{n+1}$ and $\Delta_{NL} \overline{u}_i^{n+1}$ are incremental velocity fields resulted from the time integration of linear and non-linear terms respectively. The incremental velocity field $\Delta_{NL} \overline{u}_i^{n+1}$ has frequencies beyond the characteristic frequency that defines $\overline{u}_i$ and thus should be filtered. This additional filtering should be explicitly performed at the end of each time step. Thus the modified time integration procedure can be schematically written as

$$\overline{u}_i^{n+1} = \overline{u}_i^n + \Delta_L \overline{u}_i^{n+1} + \overline{\Delta_{NL} \overline{u}_i^{n+1}}. \tag{11}$$

Note that the frequency content of each term on the right-hand side of Eq. (11) is limited to the bar level. Thus in advancing from time level n to $n+1$, the frequency content of the solution is not altered. This fact implies that the additional filtering of the non-linear terms is sufficient to achieve an explicit filtering of the velocity field for all time.

The explicit filtering procedure (11) automatically implies an alternative form of LES equations (Vasilyev *et al.*, 1998)

$$\frac{\partial \overline{u}_i}{\partial t} + \frac{\partial \overline{\overline{u}_i \overline{u}_j}}{\partial x_j} = -\frac{\partial \overline{p}}{\partial x_i} + \frac{1}{Re} \frac{\partial^2 \overline{u}_i}{\partial x_j \partial x_j} + \frac{\partial \overline{\tau}_{ij}}{\partial x_j}, \tag{12}$$

where $\overline{\tau}_{ij}$ denotes the alternative SGS stress

$$\overline{\tau}_{ij} = \overline{\overline{u}_i \overline{u}_j} - \overline{u}_i \overline{u}_j. \tag{13}$$

A possible drawback of this new formulation is that the Eq. (12) is not Galilean invariant unless a sharp cut-off filter is utilized (Vasilyev *et al.*, 1998). Non-Galilean invariance follows from the appearance of the term $c_j \partial(\overline{\overline{u}}_i - \overline{u}_i)/\partial x_j$, where c_j is the uniform translation velocity of the moving frame of reference. The error is seen to be proportional to the difference between the singly and doubly filtered velocity. This difference will be zero for a sharp cutoff filter, but will not vanish in the general case. The spectral content of the error is proportional to $\hat{G}(\mathbf{k})(1-\hat{G}(\mathbf{k}))$ where $\hat{G}(\mathbf{k})$ is the filter transfer function and $\mathbf{k}$ is the wave vector. This fact implies that the error is only generated in the wavenumber band where $\hat{G}(\mathbf{k})$ differs significantly from 0 or 1. Thus it is possible to minimize the error by constructing the explicit filter to be as close as possible to a sharp cut-off.

It turns out that non-Galilean invariance of Eq. (12) is not an issue if one adapts the correct physical interpretation of inhomogeneous turbulent complex geometry flows. We recall that if the filter width is non-uniform in one or more directions, it automatically implies that the LES equations *should not* be Galilean invariant in these directions (Ghosal, 1999). To ensure Galilean invariance in homogeneous directions of the flow one may use sharp cut-off filters in these directions.

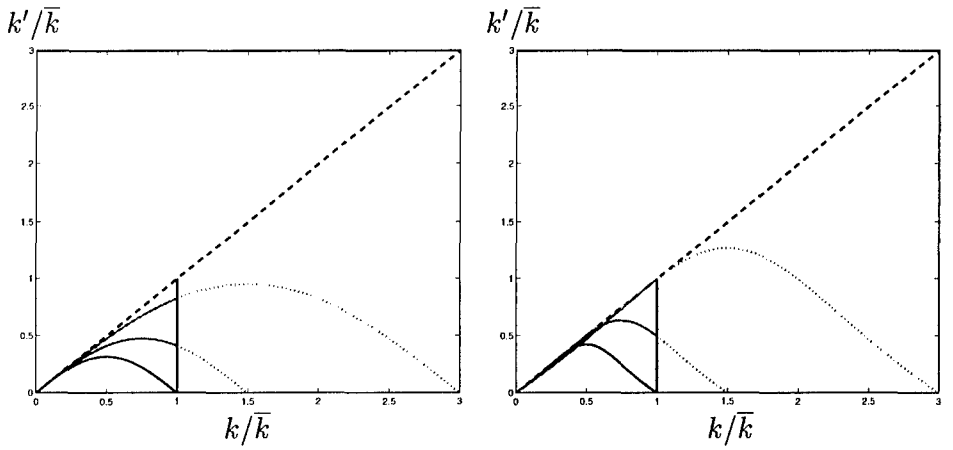

Figure 1. Modified wave-number diagram for the second (left) and fourth (right) order schemes. The vertical solid line represents the effective resolution of the explicitly filtered simulations, *i.e.* fixed cut-off frequency $\overline{k}$. The dashed line is the exact distribution that is achieved with a pseudo spectral method.

It is worthwhile to note that the use of explicit filtering provides the means for reducing the various sources of numerical error that become most severe for length scales on the order of the mesh size. By damping the high frequency portion of the solution, it is possible to control the adverse effects of numerical error. In particular, if the filter width is held fixed as the mesh is refined, the velocity field will converge to the true solution of LES equations (5) and (12). This should be contrasted to the conventional approach where the mesh is refined without the use of an explicit filter. In the latter case, additional length scales are added each time the mesh is refined, and thus the process converges to a direct numerical simulation (DNS) rather than to an LES.

It is very illustrative to consider the effect of explicit filtering on the accuracy of the solution and the computational cost associated with it in terms of modified wavenumber analysis (Lund and Kaltenbach, 1995). For simplicity let us consider the case when we filter the periodic signal given on a uniform mesh with grid size Δ_g. Then explicit filtering can be viewed as refining the mesh but keeping the same frequency content ($k \leq \overline{k}$) determined by the primary filter width Δ. The modified wavenumber diagrams for these simulations are shown in Fig.1. The solid vertical line denotes the fixed effective resolution, while the curves to the left of this line show the modified wavenumber distributions for the various values of filter width to grid ratios Δ/Δ_g. When no filter is applied (the case $\Delta/\Delta_g = 1$) considerable truncation error is evident for the upper half of the wavenumber range. As the ratio Δ/Δ_g is increased, the situation improves and the modified wavenumber slowly approaches the analytical

distribution for $k \leq \overline{k}$. Note that with the increase of the ratio Δ/Δ_g the computational cost associated with the implementation of explicit filtering also increases. Thus, in order for explicit filtering to be cost effective, the higher order schemes need to be used, since they provide the comparable modified wavenumber dependence in the range $k \leq \overline{k}$ with considerably smaller filter width to grid ratios then the lower order schemes.

In summary, the use of explicit filtering results in a LES that satisfies assumptions 2 and 3 that are used in the derivation of the LES equations. However, in order to realize the benefits of explicit filtering and satisfy assumption 1, it is necessary to develop discrete filtering operators that commute with numerical differentiation. This will be discussed next.

4. Construction of Commutative Filters

In order to realize the benefits of explicit filtering, it is necessary to develop robust and straightforward discrete filtering operators that commute with numerical differentiation. Recently a new class of *commutative* filters for both structured (Vasilyev *et al.*, 1998) and unstructured (Marsden *et al.*, 2000) grids has been developed. With these filters the differentiation and filtering operations commute to an *a priori* specified order of filter width.

We begin by discussing the continuous filtering operation and then extend it to discrete filtering. Let us consider a three dimensional field $\phi(\mathbf{x})$ $(\mathbf{x} = (x_1, x_2, x_3)^{\mathrm{T}})$ defined in a three-dimensional domain $\mathbf{D}$. The most general continuous filtering operation in physical space can be written as

$$\overline{\phi}(\mathbf{x}) = \oint_{\mathbf{D}} G(\mathbf{x}, \mathbf{y})\, \phi(\mathbf{y}) d^3\mathbf{y}, \tag{14}$$

where $G(\mathbf{x}, \mathbf{y})$ is the location dependent three-dimensional filter function. The filtering operation (14) can be substantially simplified if there exists a function $\boldsymbol{\xi} = \mathbf{f}(\mathbf{x})$ and its inverse $\mathbf{x} = \mathbf{F}(\boldsymbol{\xi})$ that maps the physical domain $\mathbf{D}$ into a rectangular domain $\Omega = [\alpha_1, \beta_1] \times [\alpha_2, \beta_2] \times [\alpha_3, \beta_3]$. In this case the filtering operation can be defined the following way: given an arbitrary function $\phi(\mathbf{x})$ we obtain the new function $\psi(\boldsymbol{\xi}) = \phi(\mathbf{F}(\boldsymbol{\xi}))$ defined in the domain Ω, the function $\psi(\boldsymbol{\xi})$ is then filtered using a sequence of three one-dimensional filters. It can be shown (Vasilyev *et al.*, 1998) that the commutation error of filtering and differentiation operations in three spatial dimensions is given by

$$\left[\frac{\partial \phi}{\partial x_k}\right] \equiv \overline{\frac{\partial \phi}{\partial x_k}} - \frac{\partial \overline{\phi}}{\partial x_k} = \mathrm{O}(\Delta_1^n, \Delta_2^n, \Delta_3^n), \tag{15}$$

provided that the filter moments $M_i^k(\xi)$ of filters G_i $(i = 1, \ldots, 3)$ exist and they satisfy the following properties:

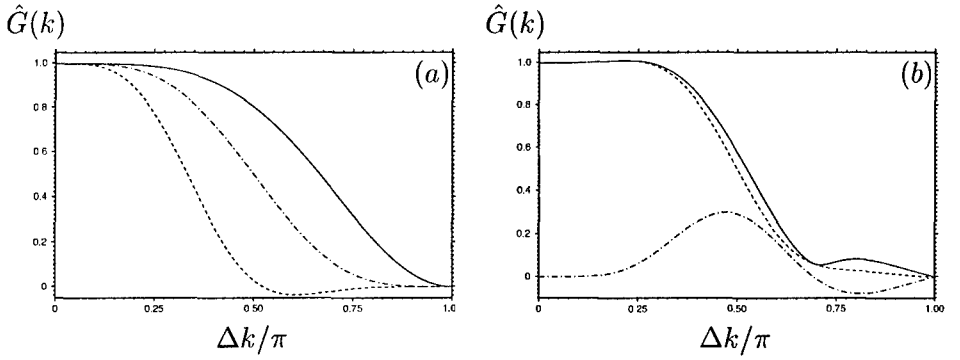

Figure 2. (a) Fourier transform $\hat{G}(k)$ of the symmetric discrete filters with three vanishing moments and different linear constraints. (b) Real, imaginary, and absolute value of $\hat{G}(k)$ of the asymmetric discrete filter with three vanishing moments.

$$M_i^0(\xi_i) = 1 \text{ for } \xi_i \in [\alpha_i, \beta_i], \tag{16}$$

$$M_i^k(\xi_i) = 0 \text{ for } k = 1, \ldots, n-1 \text{ and } \xi_i \in [\alpha_i, \beta_i]. \tag{17}$$

Also it can be shown that the commutation error in the homogeneous directions is exactly zero.

The discrete filtering operation is defined as

$$\overline{\phi}_j = \sum_{l=-K_j}^{L_j} \mathrm{w}_l^j \phi_{j+l}, \tag{18}$$

where w_l^j are the filter coefficients chosen to satisfy the zero-moment requirements (16), (17) and possibly additional constraints. Examples of discrete symmetric and asymmetric filters are shown in Fig. 2.

The discrete commutative filter construction theory can be easily extended to the case when mapped space does not exist, *e.g.* when unstructured meshes are used. In this case there is no choice, but to construct filters in the physical domain. In this case it can be shown (Marsden *et al.*, 2000) that for a smoothly varying filter width, the local commutation error in three dimensions is given by

$$\left[\frac{\partial \phi}{\partial x_1}\right] = O\left(\Delta_1^i(\mathbf{x})\Delta_2^j(\mathbf{x})\Delta_3^k(\mathbf{x})\right), \qquad i+j+k=n \tag{19}$$

provided that filters moments $M^{ijk}(\mathbf{x}) = -\int_\Psi \eta_1^i \eta_2^j \eta_3^k G(\boldsymbol{\eta}, \mathbf{x})\, d^3\boldsymbol{\eta}$ exist and satisfy the following constrains:

$$M^{ijk}(\mathbf{x}) = \begin{cases} 1 & i,j,k = 0 \\ 0 & 0 < i+j+k < n \end{cases} \tag{20}$$

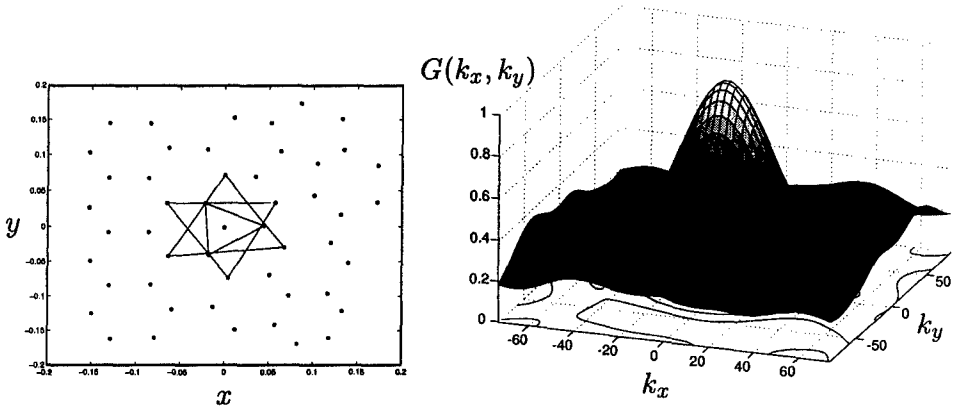

Figure 3. Example of filter constructed with triangles on an unstructured grid and the corresponding transfer function.

Greater predictability and ease of implementation can be gained by using interpolation based filters that are constructed by evaluating either interpolating polynomials (Marsden *et al.*, 2000) or least square interpolants (Haselbacher, 2001) at the desired locations. The n^{th} polynomial construction automatically guarantees an n^{th} order commutation error. To control the shape and other properties of the discrete filters, filters can be constructed as a linear combination of many polynomial based filters, while preserving the commutation properties of the filter.

In general, with an n^{th} order numerical scheme, the filtering operation must commute to order n. Most of the unstructured mesh codes are second order accurate, thus a discrete filter based on first order polynomial interpolation is sufficient to achieve second order commutation error. A two-dimensional discrete filter based on first order polynomial interpolation can be constructed using a triangle of three points surrounding the point (x_0, y_0) where we want the filtered value. A triangle is chosen because in two dimensions three points are needed for exact reconstruction of a first order polynomial. Weights are calculated by fitting a polynomial to the vertices of the triangle, and are then used to find a weighted average at the central point (x_0, y_0). With this method, the same number of points are used in the filter for any point on the mesh. Figure 3 shows an example of a 2-D filter constructed from three triangles. To achieve flexibility in filter width, each triangle as well as the central point is assigned a weight β_i, which applies equally to all vertices of the triangle. The value of β_i can be varied from 0 to 1 as long as the sum total is 1. The optimum value of β for the central point is $1/2$ because this results in a transfer function with a well defined peak and low pass filter shape.

5. Spectrum of Commutation Error

Leading order commutation error analysis described in the previous section can be viewed as a practical tool for constructing discrete filters that commute with finite difference operators to an *a priori* specified order of filter width. However, the leading order error analysis by itself is not enough to guarantee that the commutation error is negligible compared to the subgrid scale stress, since it does not use any information about spectral content of the analyzed signal (Ghosal, 1996; Ghosal, 1999). Due to the presence of significant energy in the high frequency portion of the LES spectrum, the commutation error could be considerable and in some cases even comparable with the subgrid scale stresses. The existence of inhomogeneous directions in the flow precludes the use of the standard Fourier analysis. In this section we present a recently developed mathematical tool that can be used to analyze the *local spectrum* of the commutation error and its dependence on the filter shape and the non-uniformity of the filter width.

We begin by introducing the local spectrum analysis in one-dimensional space and then extend it to three spatial dimensions. Let us consider a one dimensional filter of constant shape but variable width. The continuous filtering operation can be written as

$$\overline{\phi}(x) = \frac{1}{\Delta(x)} \int_{-\infty}^{\infty} G\left(\frac{x-y}{\Delta(x)}\right) \phi(y) dy. \tag{21}$$

Substituting the Fourier integral

$$\phi(x) = \frac{1}{2\pi} \int_{-\infty}^{\infty} \hat{\phi}\,(k)\, e^{i\kappa x} dk \tag{22}$$

into Eq. (21), changing the order of integration, and integrating the resulting equation with respect to y we obtain the following equation:

$$\overline{\phi}(x) = \frac{1}{2\pi} \int_{-\infty}^{\infty} \hat{G}\left(\Delta\,(x)\, k\right) \hat{\phi}(k)\, e^{ikx} dk, \tag{23}$$

where $\hat{G}\,(\kappa)$ is the Fourier transform of the filter function given by

$$\hat{G}\,(\kappa) = \int_{-\infty}^{\infty} G(\xi) e^{-i\kappa\xi} d\xi. \tag{24}$$

Now comparing Eqs. (22) and (23) we can see that the structure of the equations is the same. Thus, the *local* Fourier transform can be defined as

$$\hat{\overline{\phi}}(k, x) = \hat{G}\,(\Delta\,(x)\, k)\, \hat{\phi}(k). \tag{25}$$

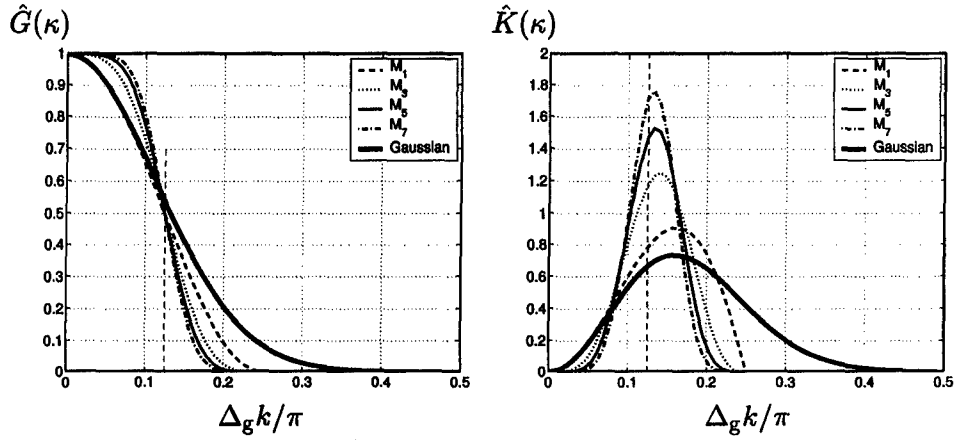

Figure 4. Transfer functions $\hat{G}(\kappa)$ and $\hat{K}(\kappa)$ for a variety of filters. M_n denotes the discrete filter with n vanishing moments.

Now the meaning of the local Fourier transform is clear, it refers to the location in space where the transform is taken and reflects the fact that the filter width is a function of location. Performing analogous analysis for commutation error it can be shown that

$$\left[\frac{d\phi}{dx}\right] = \frac{\Delta'(x)}{\Delta(x)} \frac{1}{2\pi} \int_{-\infty}^{\infty} \hat{K}(\kappa)\, \hat{\phi}(k) e^{ikx} dk, \tag{26}$$

where $\kappa = \Delta(x)\, k$ and the transfer function $\hat{K}(\kappa)$ is defined by

$$\hat{K}(\kappa) = -\kappa \frac{d\hat{G}(\kappa)}{d\kappa}. \tag{27}$$

Now the effect of filtering is clearly seen: filter width stretching affects the amplitude of the commutation error, while the filter shape and width affect the spectrum. The effect of the filter shape on the spectrum of commutation error is demonstrated in Fig. 4, where transfer functions $\hat{G}(\kappa)$ and $\hat{K}(\kappa)$ are shown for a variety of filters. It is important to note that the closer the filter to the sharp cut-off, the more localized the spectrum of commutation error. Also note that the commutation error is exactly zero, when the width of the filter is constant throughout the domain.

The one-dimensional analysis can be easily extended to three spatial dimensions. In particular, it can be shown that for three dimensional filters of constant shape and variable width the commutation error is given by

$$\left[\frac{\partial \phi}{\partial x_i}\right] = \sum_{l=1}^{3} \frac{1}{\Delta_l(\mathbf{x})} \frac{\partial \Delta_l(\mathbf{x})}{\partial x_l} \frac{1}{(2\pi)^3} \int_{-\infty}^{\infty} \hat{K}_l\left(\boldsymbol{\kappa}\right) \hat{\phi}(\mathbf{k}) e^{i\mathbf{k}\mathbf{x}} d^3\mathbf{k}, \tag{28}$$

where $\Delta_i(\mathbf{x})$ is the filter width in the x_i direction, $\mathbf{k} = (k_1, k_2, k_3)^{\mathrm{T}}$ and $\boldsymbol{\kappa} = (\Delta_1(\mathbf{x})k_1, \Delta_2(\mathbf{x})k_2, \Delta_3(\mathbf{x})k_3)^{\mathrm{T}}$ are three dimensional wave vectors,

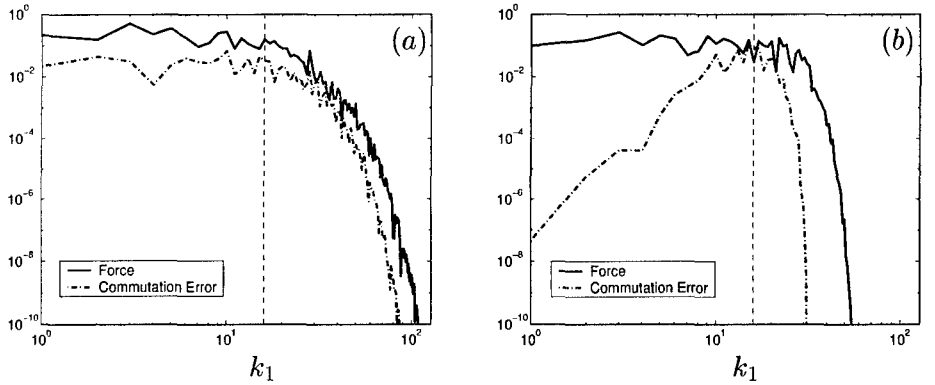

Figure 5. One-dimensional spectrum of the exact SGS force, $\partial\tau_{11}/\partial x_1$, and local one-dimensional spectrum of the commutation error for forced isotropic turbulence at $Re_\lambda = 168$ for (a) Gaussian and (b) M_7 filters.

$\hat{\phi}(\mathbf{k})$ is the Fourier transform of function $\phi(\mathbf{x})$, $\hat{G}(\mathbf{k})$ is the Fourier transform of the filter function, and the transfer function $\hat{K}_l(\boldsymbol{\kappa})$ is defined by

$$\hat{K}_l(\boldsymbol{\kappa}) = -\kappa_l \frac{\partial \hat{G}(\boldsymbol{\kappa})}{\partial \kappa_l}. \tag{29}$$

To demonstrate the effect of commutation error in LES, we consider the results of 256^3 direct numerical simulation of forced homogeneous turbulence at $Re_\lambda = 168$ (Jimenez and Wray, 1993). Figure 5 shows the one-dimensional spectrum of the exact SGS force, $\partial\tau_{11}/\partial x_1$, and the local one-dimensional spectrum of commutation error for the Gaussian and the discrete M_7 filter. These two filters are chosen because the Gaussian filter is smooth, while the M_7 filter is close to the sharp cut-off filter. The exact SGS force is obtained by filtering the DNS data. Note that the local spectrum of the commutation error shown in Fig. 5 does not take into account the grid stretching factor. The results confirm strong dependence of the spectrum of commutation error on the filter shape: the spectrum is global for smooth filters like Gaussian, while for filters, that are close to the sharp cut-off, the spectrum is localized.

6. Conclusions

In this paper we presented a systematic approach for large eddy simulation to be consistent, *i.e.* to satisfy all the assumptions used in the derivation of the LES equations. We demonstrated that a solution, consistent with the true filtered Navier-Stokes equations, can be achieved by means of explicit filtering. We have shown that explicit filtering not only provides the means for both assessing and minimizing the effects of numerical error in

practical simulations, but also allows the filter shape and size to be chosen independently of the computational mesh. Having the ability to control the filter shape opens whole new horizons in LES modelling, since it makes it feasible to look at SGS modelling and filtering as one inseparable issue. The success of explicit filtering strongly depends on the ability to construct discrete filters that commute with differentiation. We have described the general theory of construction of such filters and developed a tool for assessing the local spectrum of the commutation error.

Although tremendous progress has recently been made in the development of the explicit filtering approach, a lot of fundamental research needs to be done before researchers and engineers can take full advantage of this new mathematical tool. Among the issues which definitely need to be addressed in the near future are the development of the SGS models that correspond to specific filters and their subsequent verification with experimental and DNS results.

Acknowledgements

The author would like to thank Thomas Lund and Daniel Goldstein for their input and helpful comments.

References

Germano, M., U. Piomelli, P. Moin, and W. Cabot (1991), A dynamic subgrid-scale eddy viscosity model. *Phys. Fluids A* **3**(7), 1760–1765.

Ghosal, S. (1996), An analysis of numerical errors in large eddy simulations of turbulence. *J. Comp. Phys.* **125**, 187–206.

Ghosal, S. (1999), Mathematical and Physical Constraints on Large-Eddy Simulation of Turbulence. *AIAA Journal* **37**(4), 425–433.

Ghosal, S., T. S. Lund, P. Moin, and K. Akselvoll (1995), A dynamic localization model for large-eddy simulation of turbulent flows. *J. Fluid Mech.* **286**, 229–255.

Haselbacher, A. (2001), Discrete Filtering on Unsructured Grids Based on Least-Square Gradient Reconstruction. In: *Proceedings of the Third AFOSR International Conference on DNS/LES.*

Jimenez, J. and A. A. Wray (1993), The structure of intense vorticity in isotropic turbulence. *J. Fluid Mech.* **255**, 65–90.

Lund, T. S. (1997), On the use of discrete filters for large eddy simulation. *Center for Turbulence Research Annual Research Briefs* pp. 83–95.

Lund, T. S. and H.-J. Kaltenbach (1995), Experiments with explicit filtering for LES using a finite-difference method. *Center for Turbulence Research Annual Research Briefs* pp. 91–105.

Marsden, A., O. Vasilyev, and P. Moin (2000), Construction of commutative filters for LES on unstructured meshes. *Center for Turbulence Research Annual Research Briefs* pp. 179–192.

Rogallo, R. and P. Moin (1984), Numerical simulation of turbulent flow. *Ann. Rev. Fluid Mech* **16**, 99–137.

Vasilyev, O., T. Lund, and P. Moin (1998), A general class of commutative filters for LES in complex geometries. *J. Comp. Phys.* **146**, 105–123.